Analog Radio-over-Fiber Solutions in Support of 5G

D. Apostolopoulos, G. Giannoulis, N. Argyris, N. Iliadis, K. Kanta and H. Avramopoulos

School of Electrical and Computer Engineering, National Technical University of Athens, Athens, Greece

apostold@mail.ntua.gr

***Abstract*— We introduce Centralized (C-RAN) architectures combined with analog optical transport schemes to realize high-speed lanes between BBU pool and RRHs. The DSP-enabled architecture relies on the use of a powerful digital engine supporting data plane functions for both fiber-wireless parts. The presented concept is also supported through preliminary experiments demonstrating the proof-of-concept operation of a Fiber-Wireless link. IFoF/mmWave transmission of single-band radio signals at 60-GHz is demonstrated for Downlink directions using QAM-modulated signals at 1 Gbaud.**

Keywords—5G, Centralized-RAN, Mobile Fronthaul, Analog RoF, Millimeter Wave Radio, DSP-enabled BBU, Digital Pre-compensation/Equalization, M-QAM

I. INTRODUCTION

We have reached a critical point where the first wave of 5G compliant technologies and architectures have escaped research laboratories and are now on the verge of commercial exploitation [1]. In this context, 4G-Long Term Evolution (4G-LTE) mobile ecosystem is in the start of a transformation journey, triggered by 5G hallmarks such as millimeter waves, massive Multiple-Input and Multiple-Output (MIMO) and beamforming [2]. This transitionary phase of the entire deployed ecosystem, imposes also the process of mutation for the optical solutions which currently support the data transport within LTE networks [3]. In this way, traditional optical transport concepts supporting the Mobile Fronthaul (MFH) are expected to be replaced with new ones, capable to meet 5G requirements [4]. In more detail, current fronthaul exploits digitized optical transmission, a technique that results in a 10x bandwidth demand than the respective wireless bit-rates [5]. This digital approach can simply not scale with the increasing radio bit-rates and number of antennas required by 5G network densification approaches. Industrial consensus seems currently to agree that short- to mid-term solutions can come within digital MFH, but the required maximization of bandwidth utilization, offered by Analog Radio-over-Fiber (A-RoF) transmission, renders the transition towards concepts based on analog optics an attractive longer term 5G solution. [6].

In this work, the concept of Digital Signal Processing (DSP)-assisted optical transmission capable to support analog MFH is discussed. This RoF concept aims to alleviate the bandwidth limitations of the 5G MFH through the use of analog optics, which can carry native wireless data signals via installed fibers. We introduce this ambitious analog concept within the 5G landscape emphasizing on the structural changes and challenges that analog MFH attempts to address. In the next paragraphs, we thoroughly discuss the architectural shift towards Centralized Radio Access Network (C-RAN) topologies, which put the traditional digital MFH transport on the question. The DSP-enabled Analog architecture supporting the MFH is then presented, focusing on the digital functions undertaken from a powerful centralized DSP engine. Preliminary experiments that provide a proof-of-concept validation of our A-RoF concept are also discussed.

II. MOBILE NETWORK EXPANSION AND CENTRALIZED TOPOLOGIES

A. The transition towards C-RAN architectures

The exponential growth of the number of femto-cells to meet the demands of mobile traffic is one of the prominent features of 5G architectures that are still under investigation. To support low latency, high capacity, cost-effectiveness and low energy consumption, the entire end-to-end network should be overhauled. Currently, many Mobile Network Operators (MNOs) operate using a Distributed Radio Access Network (D-RAN), in which the 4G radio at the macro site tower consists of a collocated Baseband Unit (BBU) at the base of the tower [7]. The main advantage of D-RAN is the efficient use of backhaul bandwidth which can be achieved through various well-established technologies (Ethernet, Passive Optical Network (PON), etc.) [8]. However, dense 5G cellular topologies apply significant pressure on the static nature of D-RAN where BBUs are assigned statically to a number of cells. The spatial and temporal volatility of mobile traffic, makes the static D-RAN topologies suboptimal and new flexible topologies are needed to obtain energy and cost savings for the MNOs [9].

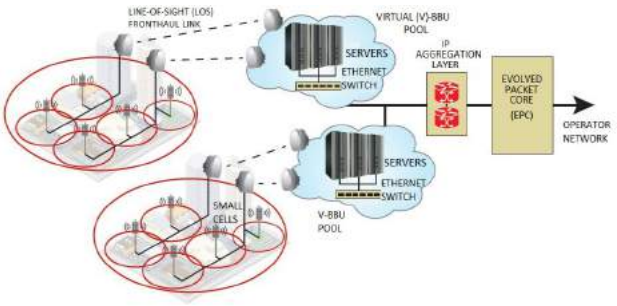

Figure 1: C-RAN architecture that has been proposed from Fujitsu for mobile scenarios within dense urban environment [7].

978-3-903176-07-2 © 2018 IFIP

Following this rational, the idea of centralization has been re-invented in the era of 5G networks, since it presents significant offerings compared to traditional D-RAN topologies [10]. The C-RAN approach favors the separation of radio elements of the base station (called Remote Radio Heads, RRH) and the elements processing the base band signal (called BBUs), which are centralized in a single location or even virtualized into the cloud. This approach, which has become a hot research topic in both academia and industry [11], benefits from simpler radio equipment at the network edge, easier to operate and cheaper to maintain, while the main RAN intelligence (BBUs) is centralized in the operator-controlled premises. The centralization is further enhanced with cloud computing [9], providing elasticity, and virtualization with possibility for multitenancy among MNOs. Several main 5G use cases, such as Virtual Reality (VR) applications, which require the real-time processing of massive amount of data, can push much of the processing from a local server to the cloud [12]. This practically means that the computational resources can be pooled and dynamically allocated to a virtual BS, which brings cost-effective hardware and software design [13]. Figure 1 provides a practical implementation of the above architecture showing a small-cell based C-RAN approach proposed from Fujitsu in a dense urban environment [7]. Beyond the software-centric solutions, the C-RAN approach needs also a paradigm shift on the hardware side to meet the challenges for the centralized baseband processing that serves a large number of RRHs. At the heart of this change, powerful Field Programmable Gate Array (FPGA) boards can offer the capability to implement high-throughput 5G transceivers for the data plane while they can also realize the Software Defined Network (SDN) functions described above for the software-centric architecture [14]. It should be noted that since the D-RAN remains the dominant deployed architecture of the antenna sites, research efforts should be considered that target a smooth transition towards 5G RAN ecosystem, supporting the coexistence of D-RAN and future C-RAN topologies [15].

B. Optical transport for MFH

The fronthaul mobile traffic transport between the BBUs and RRHs seems to be a significant challenge for 5G topologies, since it needs to address several issues related to the convergence of optical channels with complex radio interfaces. In the current C-RAN architecture designed for the Long-Term Evolution-Advanced (LTE-A) mobile network, the fronthaul interface is based on Common Public Radio Interface (CPRI). This Digitized-RoF (D-RoF) interface which relies on a link transmitting In-phase and Quadrature (IQ) data of the baseband signal components, suffers from low bandwidth efficiency since it uses the available bandwidth to send IQ data samples, decreasing thereby the effective data rate of the transport [16]. In this context, several solutions have been proposed to overcome this bandwidth wall, which mainly focus on compressed CPRI techniques with minimal impact on the optics and fiber network. The emerging need for fronthaul compression has been addressed in the current LTE-A fronthaul links, through a large set of CPRI compression algorithms [17]. Compressed CPRI links in a high-speed Pulse-Amplitude-Modulation-4 (PAM-4) are actively investigated, offering a 2x rewards on bandwidth efficiency of the D-RoF approach [18].

The CPRI compression techniques offer remarkable bandwidth gains without any structural shift on the current C-RAN architectures. However, the cost of increased complexity at the BBU side needs to be considered, while bandwidth limitations still come from digital electronics and their interfaces at the BBU side [19]. To overcome this challenge, Physical (PHY) functional split has been proposed as a possible solution for the MFH by shifting some DSP operations from BBUs to RRHs. This functional split between BBU and RRH relaxes the BBU digital overloading and lowers the fronthaul bandwidth requirements on the optical link. However, it faces great challenges when advanced coordination functionalities are required for a large number of RRHs while the latency budget is also affected through extra processing burden [20] [21]. An alternative D-RoF concept can be implemented through Open Base Station Architecture Initiation (OBSAI) which is also implemented through a packet-based interface [16]. Since the mapping methods of CPRI are more efficient than OBSAI [22], most global vendors and MNOs have chosen CPRI for deployed C-RAN topologies.

A-RoF revolutionizes the MFH landscape by fully releasing the bandwidth capabilities of mmWave bands, requiring only simple functions to exploit the offered bandwidth of the fronthaul part. Moreover, Analog MFH implementations for 5G services can harmonically co-exist over the installed fiber infrastructure supporting PON topologies of fixed wireline services [23][24]. These unique benefits come at a cost of increased hardware complexity at the BBU since it hosts the entire set of DSP functions. In addition, the optical distribution of radio signals over Intermediate Frequency/Radio Frequency (IF/RF) carriers is susceptible to a number of generation and transmission impairments, which in turn add noise and distortion due to channel nonlinearities [25].

The A-RoF approach described in the current document aims to address the above challenges through the use of powerful DSP engines implemented at ultra-high-speed FPGA boards. The proposed DSP-assisted A-RoF solution, proposes a structural shift in the current MFH deployments since it aims to combine the implementation of DSP-based functions for ultra-broadband radio signals (covering the entire unlicensed 57-64 GHz band) with the electro-optic conversion and transmission through installed fiber infrastructure.

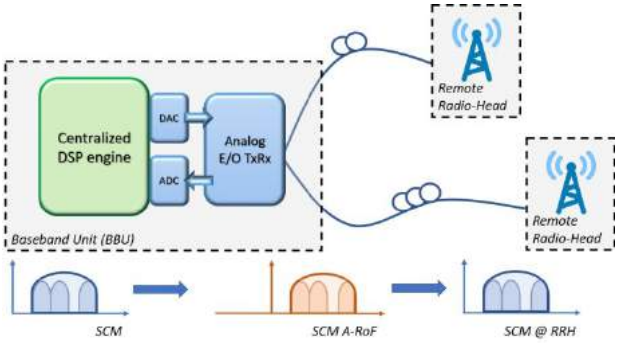

Figure 2: DSP-enabled Analog-RoF concept.

C. DSP assisted A-RoF fronthaul

Several studies explore the advantageous approach of DSP assisted A-RoF fronthaul approach. In the technique presented in [26] a number of IQ data channels, each of them corresponding to a single CPRI stream, are multiplexed and transmitted through the fronthaul link in an Intermediate Frequency-over-Fiber (IFoF) scheme. Such implementations combine commodity optical transceiver modules, carrying low bandwidth components (~10 GHz), with high speed Digital to Analog Converters (DACs) and Analog to Digital Converters (ADCs) [27]. Build upon this concept, an A-RoF architecture with DSP functionalities is presented in Fig. 4. The core of the proposed BBU architecture is a centralized DSP engine, which is responsible for implementing the physical layer functionalities for the fronthaul link. The set of these functions covers all the necessary coding/decoding, modulation and MIMO processing of the wireless channel signals. These radio signals are generated by high-performing DACs, first transmitted through the installed fiber and eventually over the air interface at the mmWave frequency band. Such an A-RoF/mmWave Fronthaul approach realizes actual centralized-RAN, since the complete set of baseband operations are digitally performed in the BBU, removing thereby any processing stage from the RRHs. A first advantage of this approach is the advanced implementation of inter-cell coordination. As the baseband processing for the radio signals to/from different RRHs is done at the same engine, tighter coordination of neighboring antennas becomes more feasible. As an example of advanced inter-cell cooperation, it is possible that two (or more than two) radiowave signals are jointly received and processed in the BBU pool so that so-called network MIMO can be achieved. Moreover, it ensures scalability since many RRHs can be placed when the capacity demands are increased in a plug-and-play manner. Besides, advanced inter-cell coordination enables better management of interference between adjacent cells, a critical point for 5G ultra-dense cellular networks [28]. Finally, the centralization of DSP engine in the BBU pool can also offer significant energy and cost savings using coordination schemes among them [29], while the hardware resources at the RRH side are practically minimized.

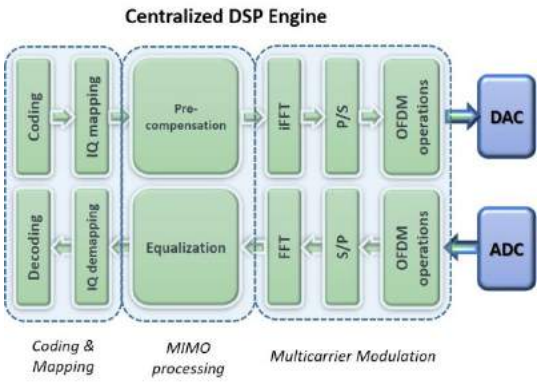

Figure 3: Centralized DSP engine for 5G-compatible Analog MFH.

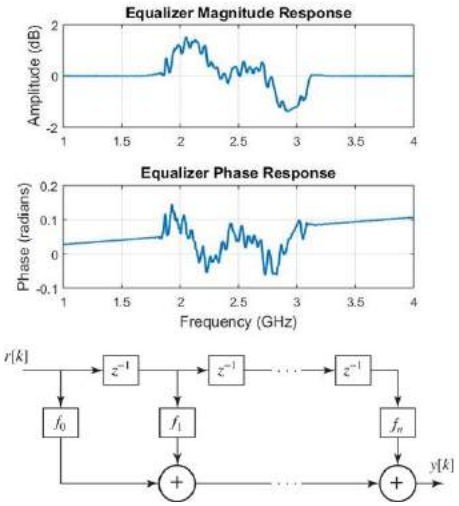

Figure 4: FIR equalizer is implemented by the Frequency Response of the A-RoF link.

III. A-RoF for MFH using a Centralized DSP Engine

A. Centralized DSP engine

Looking into more detail on the core blocks of the centralized DSP engine, the one that lies closer to the RRH is the Modulation and Channel Mapping block. In this stage, the digital sequences are mapped into the appropriate waveforms that will be transmitted over the Fiber/Wireless link. Digital modulation techniques support the generation of any Single-Carrier (SC) or Multi-Carrier (MC) scheme (e.g. Orthogonal Frequency-Division Multiplexing (OFDM)-like waveforms), thus allowing for compatibility with the current LTE standards, future upgrade to 5G candidate waveforms (eg. Universal-Filtered Multi-Carrier (UFMC), Filter Bank Multi-Carrier (FBMC), General Frequency-Division Multiplexing (GFDM) [30]) as well as more forward-looking approaches thanks to the arbitrary waveform generation capabilities of the engine. A higher bandwidth efficiency is achieved compared to D-RoF approaches of CPRI and Physical Layer Split (PLS) where the bandwidth is utilized for serial transmission of digitized IQ waveforms. In the A-RoF scheme low Intermediate Frequencies (~5 GHz) are employed to carry the modulated radio signals, resulting in bandwidths which are accommodated by typical low-cost transceivers.

Moreover, the use of Digital Sub-Carrier Multiplexing (SCM) techniques can also be adopted to further increase the bandwidth efficiency. For the SCM generation, digital upconversion schemes are employed to obtain the appropriate IF frequencies for A-RoF transmission, eliminating the need of external analog mixers and local oscillators. An additional advantage of employing SCM schemes, we fully utilize the bandwidth offered by the A-RoF components.

As the "DSP-free" RRH units are not capable of baseband signal processing, the centralized DSP engine serves on a two-fold dimension. For the downlink direction, digital pre-distortion based on the fiber/wireless channel response is performed. Channel estimation methods based on training sequences determine the magnitude and phase response of the Fi-Wi link. Thus, the response of electrical and optical components such as DACs, RF drivers, modulators, filters and photoreceivers of the optical part and RF mixers, up/down

converters of the antenna subsystem is reversed using linear equalizers implemented with Finite Impulse Response (FIR) filters. Fig. 4 illustrates a channel response extracted by a real experimental testbed with both optical and RF frontends. In the uplink, equalization stages are enhancing the demodulation and detection of the received radio signals after Wireless/Fiber transmission.

Since the A-RoF based MFH scheme appears to be significantly more efficient D-RoF approaches, accommodation of multiple RRHs' traffic can be achieved. In the special case where two or more RRHs serve the same small cell or coverage area, the DSP engine can be employed to perform equalization utilizing the spatial channel characteristics and antenna diversity, thus realizing a DSP MIMO system. Such MIMO processing capabilities along with robust coding schemes offer significant reduction in operational margins in terms of required Signal-to-Noise-and-Interference-Ratio (SNIR) and received power levels [31].

The implementation of the above rich digital portfolio within the centralized BBU will be undertaken by powerful FPGA boards. The use of these powerful FPGAs is to accelerate the critical functions of the baseband chain and sustain the necessary throughput to meet the bitrate and latency requirements within 5G. Since the FPGA boards becomes the essential part of the envisaged digital engines, the design, implementation and validation of real-time testbeds has became a significant point of interest for the 5G hardware research community [32][33]. Through the literature, several works have been conducted setting key specifications for FPGA implementation and proposing efficient implementations to meet the 5G network goals [34][35].

IV. Preliminary Experiments & Results

In this section we present preliminary experiments based on the DSP-assisted A-RoF concept described above. Figure 5(a) depicts a standard Intensity Modulation/Direct Detection (IM/DD) testbed where the A-RoF link is emulated.

An Arbitrary Waveform Generator (AWG) was used to provide the DSP functionalities for the downlink part of the Analog MFH. The programmable data source allowed Transmitter (Tx)-side DSP operations such as pulse shaping (using Root Raised Cosine (RRC), implementation of digital filters and digital pre-distortion of the optoelectronic components as described in Section III. To this end, channel estimation has been performed, prior the actual data transmission, where an amplitude and phase channel response was estimated on the frequency domain. Through the AWG, the pre-distorted data signals were digitally upconverted to the selected IF. This mixerless scheme was based on the use of embedded DAC of the AWG without the need of any external analog RF signals. A single-drive electro-optic modulator was used to generate the IFoF signal carrying the radio bands with the intensity modulator biased at the quadrature point ($V_\pi/2$). The Mach-Zehnder Modulator (MZM) was biased at the quandrature point to ensure its operation at the linear regime of transfer function.

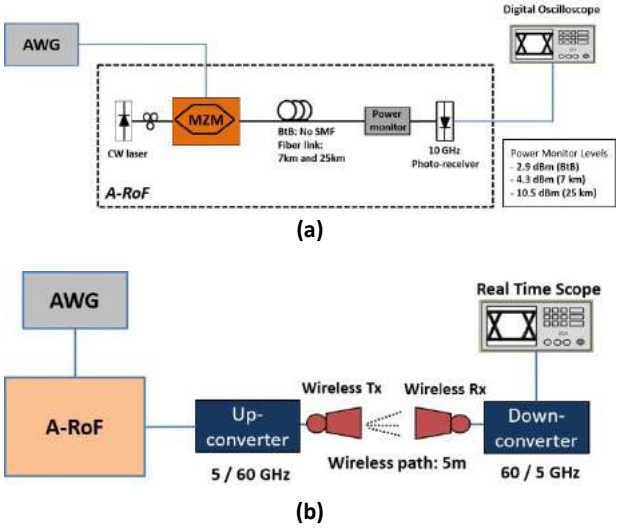

Figure 5: (a) A-RoF testbed on an IM/DD link using laboratory equipment (b) Fiber-Wireless link

Fiber links of Standard Single-Mode Fiber (SSMF) up to 25 km were used in the testbed to emulate the fiber connection between the BBU and RRHs. At the receiver side, commercial off-the-shelf 10 GHz photo-receiver allowed for the optical-to-electrical conversion and the efficient interface with the radio hardware. Figure 5(b) illustrates the above emulation of a converged Fiber-Wireless link where the A-RoF output is connected directly to V-band radio hardware. The received IF signal was up- and down-converted via commercially available V-band upconversion modules with Local Oscillator (LO) operated at 58-63GHz. Standard pyramidal gain horn V-band antennas of 23 dBi gain and 10° beamwidth were employed. These directional antennas together with the up- and downconversion units, were mounted on wooden tripods and kept fixed at a height of 1.4 m above the floor located in a 5 m horizontal distance in an indoor laboratory environment.

Single-Band and Multi-band transmission experiments were carried out considering initially only the fiber part and then, the Fiber-Wireless link. An IF frequency of 5 GHz was selected in order to meet the specifications of the mmWave Up- and Down-converter units at the radio part. Such selection easily accommodates the entire bandwidth (~7GHz) within the targeted unlicensed radio band and provides resilience against the power fading due to Chromatic Dispersion (CD) for fiber lengths up to 25 km [36]. Moreover, since IF frequencies were employed to balance the bandwidth gap between the electronic and photonic devices, the need for high speed optical frontends is eliminated.

Exploiting once more the DSP capabilities on generation of complex waveforms, four different subcarriers have been digitally synthesized, before feeding a single DAC board in order to generate the desired multiband radio signal. The 4 sub-bands were assigned at 0.625 GHz, 1.875 GHz, 3.125 GHz and 4.375 GHz center frequencies (around 2.5 GHz) and each of them was modulated at 1 Gbd symbol rate, pulse-shaped with a RRC filter ($\alpha = 0.2$), utilizing thereby a total 5 GHz bandwidth. Different modulation types were investigated for the sub-bands. Figure 6(a) shows that in the case of back-to-back measurement, all sub-bands have almost the same performance and the modulation type does not affect the measured Error Vector Magnitude (EVM) values. After fiber transmission over the 25-km fiber link, the effect of dispersion-induced power fading is evident, since the higher frequency components suffer from severe distortion compared to lower. The use of a higher order modulation format seems

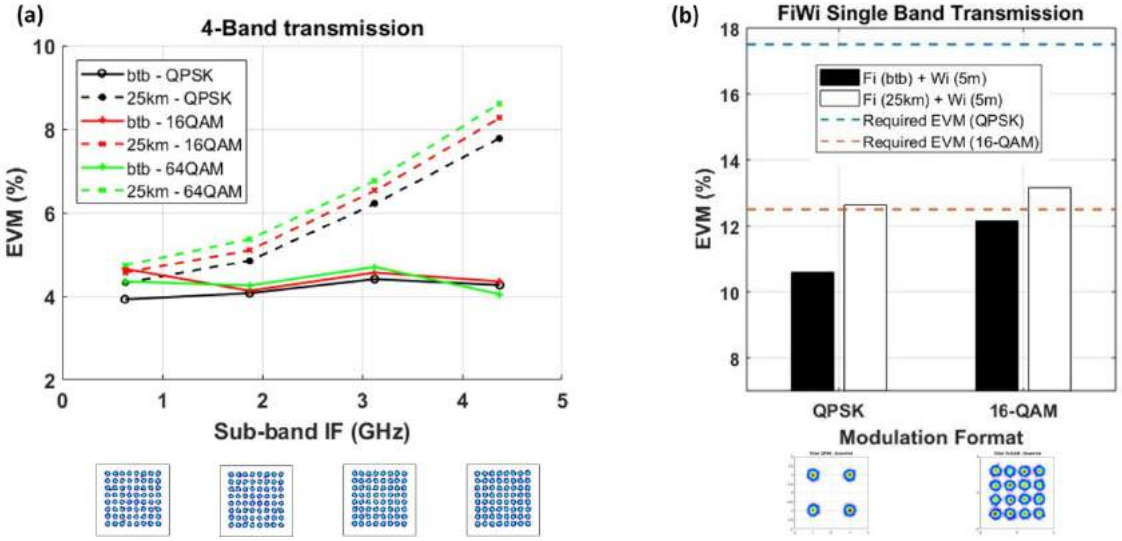

Figure 6: (a) EVM measurements for each sub-band of the SCM A-RoF link (a) 4-bands, Constellation diagrams for 64-QAM after 25km, (b) EVM bar-diagram measurements for A-RoF/mmWave transmission in downlink directions. Constellation diagrams for QPSK and 16-QAM after Rx-side DSP are also included.

to slightly increase the EVM value, which does not hamper the demodulation of this formats in this specific case. EVM values below 8.5% were achieved for all QPSK, 16-QAM and 64-QAM schemes in all the allocated spectrum bands. A total data transport rate for 64-QAM modulation type of 24 Gb/s can be achieved.

Comparing the EVM performance between the single band and multiple band IFoF transmission, it is evident that the signal distortion is increased for increased number of radio bands as it is expected. Moving towards wide-band, multi-carrier approaches, the analog photonic links suffer from cross modulation distortion (XMD) which introduces severe distortion in the modulated in-band of each signal [37].

The next evaluation step comprises the characterization of fiber-wireless link including both fiber and wireless part. Combining the proposed A-RoF IM/DD optical fronthaul topology with commercial V-band radio hardware (operated at 57-64 GHz unlicensed band), indoor wireless measurements using directional antenna elements were performed.

For the DL operation the signal after the transmission through the A-RoF link was received by a photoreceiver (Avalanche Photodiode Photoreceiver (APD) + Transimpedance Amplifier (TIA)). This modulated IF output is fed into a mmWave upconverter to obtain the mmWave transmission through the air. After the digitization of the received signals, digital downconversion from the IF frequency to baseband was performed. There, matched filtering, resampling and proper timing synchronization was applied in order to extract a single-sample per symbol sequence. For the equalization stage, a static 5-tap Radius Directed Constant Modulus Algorithm (CMA) algorithm was employed for off-line equalization of both fading effects stemming from both fiber-air transmission and to remove the frequency response from mmWave components. Finally, a Carrier Phase Recovery stage compensated for the phase noise due to local oscillators' mismatches. Statistical constellation analysis and error counting was employed for estimating and measuring the transmission quality. In this experiment Single-CarrierQuadrature Phase Shift Keying (QPSK) and 16-QAM) at 1 Gbd symbol rate were employed as modulated radio signals. A RRC pulse shaping filter with 20% excess bandwidth resulted a total 1.2 GHz to be transmitted through the fiber/wireless link. In Figure 6(b), we present an EVM bar diagram for both uplink and downlink operation using the above modulation types. In order to investigate the role of fiber transmission, the long fiber-part of 25 km was also used for the measurements. The reported results show that the fiber part of 25 km introduces severe signal distortion which leads to higher EVM values compared to back-to-back measurements, as it was originally expected. The calculated EVM value after the fiber wireless transmission was measured to be just above the limit value, according to 3GPP standards, for successful 16-QAM signal demodulation [38]. As a future step, the use of channel estimation techniques and improved equalization algorithms could offer even lower EVM values, to meet the 3GPP requirements for 16-QAM modulation type.

V. Conclusion

This work presented a DSP-enabled concept that can efficiently support the MFH of C-RAN architectures. Through literature review, the shift towards 5G centralized topologies was introduced while the optical transport was addressed via bandwidth efficient A-RoF concept. The DSP engine, responsible for the data plane functions, was thoroughly discussed focusing on the efforts to host the complete set of digital functions at the BBU side, real-time implemented via powerful FPGA boards.

In this work, results from preliminary experiments are also included aiming at the verification of the proposed A-RoF solution for realistic fronthaul scenarios. The optical transport of multiband radio signal carrying 64-QAM modulated signals was experimentally demonstrated showing EVM values below 8.5%. The wireless transmission was achieved by connecting radio equipment at 60GHz. We experimentally demonstrated fiber-wireless transmission link up to 4 Gb/s using QPSK and 16 QAM modulation types which exhibited EVM values below 13% for both cases.

Acknowledgment

This work has been supported by the European Commission through H2020 5GPPP Phase II project 5G-PHOS, Contract Number 761989.

REFERENCES

[1] A"5G Cell Service Is Coming. Who Decides Where it Goes?", article appeared at online version of www.nytimes.com, posted at 2018-03-02 by Allan Holmes.

[2] E. Larsson, O. Edfors, F. Tufvesson, and T. Marzetta, "Massive MIMO for next generation wireless systems, " IEEE Commun. Mag., vol. 52, no. 2, pp. 186–195 (2014).

[3] N.J. Gomes et al., "The new flexible mobile fronthaul: digital or analog, or both?", in Proc. of International Conference on Transparent Optical Networks (ICTON 2016), 10-14 July 2016, Trento, Italy.

[4] M. Presi et al., "Optical Solutions supporting 5G and Beyond", Presentation slides uploaded in the 5G-PPP repository, 23 March 2016.

[5] T. Pfeiffer, "Next generation mobile fronthaul and midhaul architectures," J. Optic. Comm. Netw., Vol. 7, Issue 11, pp. B38-B45 (2015).

[6] J. Kani, J. Terada, K.-I. Suzuki, A. Otaka, "Solutions for Future Mobile Fronthaul and Access-Network Convergence," IEEE Journal of Lightwave Technology, Vol.35, Issue 3, pp.527-534 (2017).

[7] "The Benefits of Cloud-RAN Architecture in Mobile Network Expansion", Application Note from Fujitsu Network Communications Inc. (2014).

[8] Agata and K.Tanaka, "NG-EPON for Mobile Access Network", presented in IEEE 802 Plenary Session, March 2014, Beijing, China.

[9] A. Checko et al., "Cloud RAN for Mobile Networks – A Technology Overview", IEEE Communications Surveys & Tutorials, Vol.17, Issue 1, pp. 405-426 (2015).

[10] China Mobile Research Institute, "C-RAN: The Road Towards Green RAN," White Paper, 2013. Available: http://labs.chinamobile.com/cran/

[11] Manli Qian et al, "A super base station based centralized network architecture for 5G mobile communication systems", Digital Communications and Networks (2015).

[12] M. Koziol, "Mobile World Congress 2018: Don't Expect 5G Service Anytime Soon", posted in spectrum.ieee.org, 2 March 2018. https://spectrum.ieee.org/tech-talk/telecom/wireless/mobile-world-congress-2018-5g-isnt-for-you

[13] D. Wubben et al., "Benefits and impact of cloud computing on 5G signal processing: Flexible centralization through cloud-RAN," IEEE Signal Process. Mag., vol. 31, no. 6, pp. 35–44, Nov. 2014.

[14] M. Milosavljevic, "FPGAs for Reconfigurable 5G and Beyond Wireless Communication", presented in NMI FPGA Network: "Safety, Certification and Security", University of Hertfordshire, 19 May 2016, Hatfield, UK.

[15] C. Raack, J.M. Garcia, R. Wessaly, "Centralized versus Distributed Radio Access Networks: Wireless intergation into Long Reach Passive Optical Network", in Proc. of CTTE 2015, 9-10 November 2015, Munich, Germany.

[16] A. Olivia et al., "An Overview of the CPRI specification and its application to C-RAN based LTE scenarios", IEEE Communications Magazine, Vol. 54, Issue 2, pp. 152-159 (2016).

[17] White paper from Altera. "The Emerging Need for Fronthaul Compression", June 2016.

[18] F. Lu et al. "Adaptive Digitization and Variable Channel Coding for Enhancement of Compressed Digital Mobile Fronthaul in PAM-4 Optical Links", IEEE Journal of Lightwave Technology, Vol.35, No.21,pp.4714-4720 (2017).

[19] N. Carapellese et al, "BBU placement over a WDM aggregation network considering OTN and overlay fronthaul transport,," European Conf. on Optical Com. (ECOC), pp. 1-3, 2015

[20] K. Miyamoto, S. Kuwano, J. Terada, and A. Otaka, "Split-phy processing architecture to realize base station coordination and transmission bandwidth reduction in mobile fronthaul," presented at the Optical Fiber Communications Conf. Exhib., Los Angeles, CA, USA, 2015, Paper M2J.4.

[21] J. Armstrong, "OFDM for Optical Communications," Journal of Lightwave Technology, vol. 27, no. 3, pp. 189-204, Feb.1, 2009.

[22] M. Nahas, A. Saadani, J. Charles, and Z. El-Bazzal, "Base stations evolution: Toward 4G technology," in Telecommunications (ICT), 2012 19th International Conference on. IEEE, 2012, pp. 1–6.

[23] X. Hu, C.Ye and K.Zhang, "Converged Mobile Fronthaul and Passive Optical Network Based on Hybrid Analog-Digital Transmission Scheme", in Proc. of Optical Fiber Communications Conf (OFC) 2016, paper No. W3C.5, 20-24 March 2016, Anaheim, CA, USA.

[24] G. Kalfas et al., "Non-Saturation Delay Analysis of Medium Transparent MAC Protocol for 60 GHz Fiber-Wireless Towards 5G mmWave Networks," J. Lightwave Technol. 35, 3945-3955 (2017).

[25] C. Lim et al., "Mitigation strategy for transmission impairments in millimeter-wave radio-over-fiber networks", Journal of Optical Networking, Vol.8, No.2, pp.201-214 (2009).

[26] X. Liu, H. Zeng, N. Chand and F. Effenberger, "Efficient Mobile Fronthaul via DSP-Based Channel Aggregation," in Journal of Lightwave Technology, vol. 34, no. 6, pp. 1556-1564, March, 15 2016.

[27] X. Liu, H. Zeng, N. Chand and F. Effenberger, "CPRI-compatible efficient mobile fronthaul transmission via equalized TDMA achieving 256 Gb/s CPRI-equivalent data rate in a single 10-GHz-bandwidth IM-DD channel," 2016 Optical Fiber Communications Conference and Exhibition (OFC), Anaheim, CA, 2016, pp. 1-3.

[28] Nurul Huda Mahmood et al, "A centralized inter-cell rank coordination mechanism for 5G systems", 13th International Wireless Communications and Mobile Computing Conference (2017).

[29] B.J.R. Sahu, S. Dash, N.Saxena, A. Roy, "Energy-Efficient BBU Allocation for Green C-RAN", IEEE Communications Letters, Vol.21, Issue 7, pp. 1637-1640 (2017).

[30] X. Zhang, M.Jia, L.Chen, J. Ma, J. Qiu, "Filtered-OFDM – Enabler for Flexible Waveform in the 5th Generation Cellular Networks", in Proc. of IEEE Global Communications Conference (GLOBECOM 2015), 6-10 December 2015, San Diego,CA, USA.

[31] C. Masterson, "Massive MIMO and Beamforming: The Signal Processing Behind the 5G Buzzwords", Analog Devices White Paper, June 2017

[32] P. Harris, et al. "Performance characterization of a real-time massive MIMO system with LOS mobile channels." IEEE Journal on Selected Areas in Communications 35.6 (2017): 1244-1253.

[33] M. Wu, B.Yin, G. Wang, C.Dick, J.R. Cavallaro, and C.Stuper, "Large-Scale MIMO Detection for 3GPP LTE: Algorithms and FPGA Implementations", IEEE Journal of Selected Topics in Signal Processing, Vol.8, Issue 5, pp. 916-929 (2014).

[34] T.H. Pham, S.A. Fahmy, and I.V. McLoughlin. "An End-to-End Multi-Standard OFDM Transceiver Architecture Using FPGA Partial Reconfiguration." IEEE Access 5 (2017): 21002-21015.

[35] S. Malkowsky et al., "The World's First Real-Time Testbed for Massive MIMO: Design, Implementation and Validation", IEEE Access, Vol.5, pp.9073-9088 (2017).

[36] R. Hui et al., "Subcarrier Multiplexing for High-Speed Optical Transmission", Journal of Lightwave Technology, Vol.20, No.3, pp.417-427 (2002).

[37] X. Liang, et al., "Digital suppression of both cross and inter-modulation distortion in multi-carrier RF photonic link with down-conversion", Optics Express, Vol.22, No.23, pp.28247-28255 (2014).

[38] 3rd Generation Partnership Project, "Technical Specification Group Radio Access Network – NR - Base Station (BS) radio transmission and reception", V15.0.0 (2017-12).